scientific reports

Check for updates

OPEN

The Gompertz Law emerges naturally from the inter-dependencies between sub-components in complex organisms

Pernille Yde Nielsen[1]✉, Majken K Jensen[2], Namiko Mitarai[3] & Samir Bhatt[2,4]

Understanding and facilitating healthy aging has become a major goal in medical research and it is becoming increasingly acknowledged that there is a need for understanding the aging phenotype as a whole rather than focusing on individual factors. Here, we provide a universal explanation for the emergence of Gompertzian mortality patterns using a systems approach to describe aging in complex organisms that consist of many inter-dependent subsystems. Our model relates to the Sufficient-Component Cause Model, widely used within the field of epidemiology, and we show that including inter-dependencies between subsystems and modeling the temporal evolution of subsystem failure results in Gompertzian mortality on the population level. Our model also provides temporal trajectories of mortality-risk for the individual. These results may give insight into understanding how biological age evolves stochastically within the individual, and how this in turn leads to a natural heterogeneity of biological age in a population.

Facilitating healthy aging has become a major goal in medical research, as both life expectancy and incidence of age-related disease increases[1]. Although it has been pointed out that there exists an ongoing nonconcensus on defining what "biological aging" is[2], the concept of biological age can be found in literature dating back several decades[1]. Considerable effort has been made in order to define and quantify biological age and a huge number of biomarkers that correlate with age have been elucidated and combined into various quantitative measures of biological age or so-called "aging clocks"[3,4] and the related "frailty indexes"[5–7]. However the concept of biological age lacks a precise and generally accepted definition[1,8,9].

Several authors have pointed out the need for understanding the system as a whole rather than focusing on individual molecular or cellular factors[1,10]. More general features and underlying mechanisms of aging may be discovered by adopting a complex systems approach and shifting the perspective to studying the joint influence of several interacting subsystems. Elucidating hierarchical structures and patterns of interactions between subsystems may reveal how underlying mechanisms of aging emerge on larger scales. Here we focus on one of the most well-known emergent demographic mortality patterns, namely the Gompertz Law[11–13], stating that adult mortality rates increase exponentially with age:

$$\mu(t) = R_0 e^{bt} \tag{1}$$

Here $\mu(t)$ is the mortality rate, also known as the "force of mortality", "failure rate" or "hazard rate"[12,14,15] and t equals chronological age, i.e., time since birth. The Gompertz Law has two parameters: R_0 is the hypothetical mortality rate at birth, and b is the "Gompertz coefficient"[16] that determines the rate of increase of the exponential term. Apart from its application to mortality rate, the Gompertz Law is also able to describe patterns in disease incidence rates, as the risk of many diseases have been observed to increase exponentially with age with the same doubling time as risk of death[17–21]. The Gompertz Law is also observed in failure rates of computer code[22] and

[1]Department of Applied Mathematics and Computer Science, Technical University of Denmark, 2800 Kongens Lyngby, Denmark. [2]Department of Public Health, University of Copenhagen, Copenhagen, Denmark. [3]Niels Bohr Institute, University of Copenhagen, Copenhagen, Denmark. [4]MRC Centre for Global Infectious Disease Analysis, Department of Infectious Disease Epidemiology, Faculty of Medicine, Imperial College London, London, UK. ✉email: pydni@dtu.dk

in more abstract measures such as termination rates of self-avoiding random walks in a random network[23]. A key facet of Gompertzian mortality is that it is universal and is used to describe the main temporal mortality-pattern observed in many different species, with only few exceptions[12,24–26]. This universality indicates that all such species may share a common age-related dynamical trait, accounting for the pace of increasing mortality rate with age. Identifying a mechanism that drives the emergence of Gompertzian mortality would be of great value in order to understand the driving forces behind mortality, shared by all species displaying Gompertzian mortality patterns, and in order to understand the aging process itself[10,25,27]. Understanding why the mortality rate increases with age may also give insight into the field of biological age research and the possibility of inter-individual heterogeneity in the pace of aging.

Previous research has focused on mechanistic (kinetic) models that result in the emergence of Gompertzian mortality patterns, either by mimicking concrete biological processes, or through more abstract models related to reliability theory (general theory of system failure). Some of these models incorporate an explicit exponential parametric shape but do not show how this time-dependence emerges[15,16,28]. Other models have been shown to produce Gompertzian mortality, without assuming an explicit exponential parametric shape—i.e., the exponential increase in mortality rates emerges naturally from the model structure and the architecture of dynamic interactions between model variables[5,14,19,23,25,29,30]. A commonality in these models is an underlying stochastic process describing either the accumulation or depletion of a physical entity. The model introduced by Alon et. al. focuses on a specific biological component, namely senescent cells[19,29], and describes how the amount of senescent cells may increase with age due to saturation of repair mechanisms. In this model death occurs, when the density of senescent cells reaches a predefined fatal threshold. Other models describe abstract entities such as "frailty" or "vitality", and the stochastic process may therefore be interpreted as, e.g., accumulation of damage or depletion of capacity (also termed *resilience* or *redundancy*). An early approach introduced by Beard[14], named these models "forward" and "backward" models respectively, and wrote: "*In the forward model hits are assumed to accumulate and death to occur when the total reaches a certain figure. In the backward model the individual is assumed to start with a quota of units which are progressively lost in time, death occurring when the total remaining falls below a certain figure*"[14]. It is difficult to assert whether these models mimic a sufficiently generalizable system, because the modeled entity tends to be very abstract and without biological justification or a link to biological mechanisms and processes. Furthermore, both the abstract models and the more specific model by Alon et. al. assume that death occurs once the stochastic process reaches a predefined fatal threshold (or "figure" in the parlance of Beard[14]). The need for such a threshold seems undesirable as it is somewhat arbitrary and additionally conflicts with the notion that death may occur due to many different reasons. One related model to what we propose was introduced by Gavrilov and Gavrilova in 2001[25] where mortality rates are modelled via *redundancy exhaustion* in a system exposed to random initial flaws. In this model the organisms are represented by a number of irreplaceable "blocks" and each block comprises a certain number of redundant elements. The elements fail individually through a stochastic process, but since the elements in the same block represent redundancy, the entire organism only dies when an entire block is failed. The authors show that this model system produces Gompertzian mortality patterns, if the blocks are subject to random initial failures, which is equivalent to assuming a certain distribution of block sizes. This model successfully describes death as the outcome of one of many different fatal states (each "block" represents one cause of death), and shows how Gompertzian mortality may emerge from a model consisting of non-aging elements, as the failure rate of individual elements is constant. However, recent advances within the field now referred to as "Network Medicine" has underlined the notion that both pathology and mortality is rarely the consequence of a single exposure, but instead the result of biological processes that interact in a complex network of inter-dependencies (see, e.g. Barabási et. al. 2011 and references therein[31]). The strictly block compartmentalised structure of the model by Gavrilov and Gavrilova can be argued to disagree with the complex interconnected architecture of biological systems[32], as the blocks are completely independent with no inter-connections and no overlap. Another relevant model that does use a network approach is proposed by Rutenberg et. al.[5–7]. Here, each node in a scale-free network represents a "health attribute", which is subject to damage. Random damage initialising in peripheral nodes with low connectivity can therefore spread through nodes of higher connectivity, resulting in a situation where damage promotes more damage[6]. This model is also able to produce Gompertzian mortality patterns, when death is modelled as the event where the two top most connected nodes are damaged[5]. While the structure and implications of this model are relevant, the representation of death (top two nodes in combination) seems somewhat abstract.

Here, we adopt a complex systems approach and show how the Gompertz law emerges naturally from an extremely simple stochastic system. The proposed model is highly related to several of the above mentioned models, but our model is distinguished by its parsimony and incorporation of both inter-dependencies and broad range of causes of death. Our goal is to provide a general theoretical explanation for the emergence of Gompertzian mortality using a minimal set of highly plausible assumptions. We represent an individual as a collection of *subsystems*, which can fail and can trigger subsequent failures (Fig. 1). Our model describes the probability that an organism (or system) will enter one of many fatal states, agreeing with the notion that organisms may die due to many different causes. Each fatal state is described as a combination of subsystem failures and the living organism is modelled as an ensemble of *many* subsystems. We do not specify exactly what these individual subsystems are, and it is likely they could be defined on multiple levels. At any time there is an instantaneous probability (risk) that any subsystem will cease to function correctly and thereby fail. For simplicity we focus first on the special case where subsystem function/failure is modeled as a binary irreversible state, but we also show that the model can easily be expanded to include a repair mechanism.

While our model is constructed using typical methodology from systems biology and statistical physics, it can very easily be related to the widely used epidemiological *Sufficient-Component Cause Model* by Rothman[33]. Failure of an individual subsystem is equal to one *component cause*. Each fatal state—i.e., fatal combination of subsystem failures—corresponds to a *sufficient cause*. Our model describes how the number of subsystem

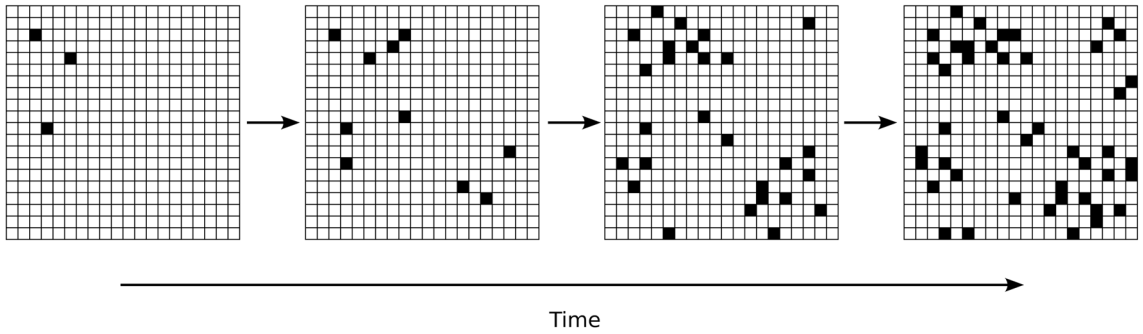

Figure 1. Accumulation of subsystem failures increase with time. An organism is schematically displayed as a system with many subsystems (individual squares). Individual subsystems may "fail" (indicated by black squares) and therefore the overall system will accumulate failed subsystems over time (number of black subsystems increases with age). Certain combinations of failed subsystems will cause death. Other combinations of failed subsystems may result in certain disease.

failures within an organism increases with time and how this in turn leads to an increased probability (risk) for the organism to die. The mortality rate for a population is then given by the average risk of death at any point in time. We show that our simple conceptual model is able to describe Gompertzian mortality patterns emerging from the following five assumptions:

1. Organisms consist of multiple subsystems, and all subsystems are at risk of failure
2. Subsystems are *inter-dependent* and failure of one subsystem will *on average* increase the failure-risk of other subsystems
3. Certain combinations of subsystem failures cause death of the entire organism. There may be *many* different combinations of subsystem failures that lead to death—reflecting different causes of death
4. The probability of obtaining a fatal combination of subsystem failures is proportional to the fraction of failed subsystems within the organism
5. Death occurs at fractions of failed subsystems which are relatively small

Taken together we term this model a "*Multiple and Inter-dependent Component Cause model*" (MICC). As the model is intended to minimize the number of assumptions, while still producing an explanation for the Gompertz Law, the five points in the above list presents a somewhat simplified representation of real biological organisms. The model is equivalent to a fully connected network in which each node is one subsystem and all edges (links) have equal strength. This is a simplification of real biological organisms, which contain detailed and highly organised but also interconnected structures—examples of larger structures could be, e.g., the cardiovascular system, the immune system, the different organs etc. The model can easily be expanded to include an explicit network structure such as scale-free or modular—both of which have been observed in real biological systems[32]—but here we choose to model the organism as a fully connected network with equal edge strengths in order to show that the explicit network structure is not required for the emergence of Gompertzian mortality. As we do not define the individual subsystems explicitly, the assumption that subsystems are inter-dependent (point 2 in the above list) also becomes a simplified representation of the true detailed structure found in real biological organisms. The assumption that failure of subsystems increase the failure-risk of other subsystems is supported by the fact that many diseases (i.e., certain combinations subsystem failures) are also risk factors for other diseases (i.e., further subsystem failures), leading to increased comorbidity[34], and also supported by the studies of "Frailty Indexes"[6,7], showing that an increased number of health deficits (i.e., certain subsystem failures) is generally associated with higher risk of disease outcomes (i.e., further subsystem failures). The assumption that certain combinations of subsystem failures lead to death (point 3 in the above list) is in line with the conceptual model of causation put forward by Rothman in 1976[35], arguing that a *sufficient cause* for an outcome (e.g., death) consists of a combination of *component causes* (here equal to subsystem failures) and that several different combinations may constitute different sufficient causes for the same outcome. While the combinations of subsystem failures that lead to death relate to the "blocks" described in the model by Gavrilov and Gavrilova[25], the model presented here includes possible overlap between different causes of death as well as correlations and inter-dependencies between the individual subsystems. Additionally, this model describes the entire set of subsystems in an organism and not only the ones that enter in possible fatal combinations. The model therefore also describes the gradual accumulation of failure that happen before death occurs. In our model, not only death, but also diseases may be described as combinations of subsystem failure.

The MICC model results in a logistical growth of the fraction of failed subsystems. This logistical growth exhibits an exponentially increasing mortality rate in the limit where the fraction of failed sub-systems is relatively small. If death of biological organisms occurs at relatively small fractions of subsystem failures (point 5 in the above list), the model thus succeeds in explaining Gompertzian mortality. Dependent on parameters, the model is also able to explain the possible "late life mortality deceleration"[26,36–38], i.e., deviation from Gompertzian mortality

at advanced ages, as the logistic growth of the mortality rate approaches the inflection point and starts to saturate. The model is also able to explain why the incidence of many diseases also increase exponentially with age[17,18].

The inter-dependency between subsystems is a key assumption in order to gain exponential increase, as this is what drives a self-amplifying process, leading to the accelerated increase in mortality rate. In the terminology of the "*Sufficient-Component Cause Model*"[33], this is equal to stating that every component cause on average will increase the risk of other component causes to occur. The addition of this simple form of interaction between subsystems is sufficient to expand the original "*Sufficient-Component Cause Model*" to explain the emergence of Gompertzian mortality patterns.

The MICC model is very simple, yet comprehensive. Its strength is the complex systems view, describing not a specific biological pathway but the overall system and the interactions between subsystems. The complexity of living organisms is captured by the large number of subsystems in the model and the notion that many (different) combinations of subsystem failure can lead to death.

Results

Multiple and inter-dependent component cause model in a *mean field* version

We consider an organism consisting of N subsystems. Ideally all N subsystems are functioning correctly, but at any time there is a risk for each individual subsystem to fail. This risk is given by the probability p. At time t the number of failed subsystems is given by $F(t)$, and the number of subsystems that are still functioning correctly is given by $M(t)$, such that total number of subsystems is conserved, i.e., $F(t) + M(t) = N$.

Within a small time-step, Δt, the number of failed subsystems will increase by $\Delta F = F(t + \Delta t) - F(t)$. The probability (risk) of failure for *each* individual subsystem is given by $p(t)$ and the number of subsystems that are at risk of failing is given by $M(t)$.

$$\Delta F = p(t) \cdot M(t) = p(t) \cdot (N - F(t)) \tag{2}$$

A constant risk of subsystem failure, $p(t) = C \cdot \Delta t$, corresponds to the case where all subsystems fail independently at a constant rate C. Such a situation will *not* result in Gompertzian mortality (see Supplemental Appendix A). Instead we describe a situation where the risk of failure depends on the amount of subsystems that have already failed, i.e., the subsystems are *inter-dependent*: failure in one subsystem increases the risk of failure in other subsystems. On *average* we have $p(t) = r \cdot F(t) \cdot \Delta t$, making the individual risk of subsystem failure proportional to $F(t)$, the number of already failed subsystems. From the above we obtain a differential equation for the average change in $F(t)$, in the limit of $\Delta t \to 0$:

$$\frac{dF(t)}{dt} = \lim_{\Delta t \to 0} \frac{\Delta F}{\Delta t} = r \cdot F(t)(N - F(t)) \tag{3}$$

The solution to Eq. (3) is a standard logistic growth curve:

$$F(t) = \frac{N \cdot F_0}{F_0 + (N - F_0)e^{-rNt}} \tag{4}$$

$F(t)$ has a sigmoidal shape: starting from the value F_0 at time zero, $F(t)$ increases exponentially at early times. The exponential increase levels off and an inflection point is reached at time, $t = \tau$, after which the increase of $F(t)$ decelerates and finally saturates at a level $F(t) = N$. See Fig. 2A.

Mortality rate in a Mean field model

According to third assumption defined in the introduction, we assume that certain combinations of failed subsystems lead to the death of the organism, but we do not specify a weighting or the explicit sets of combinations that lead to death. Instead, and according to the fourth assumption, we model the probability of obtaining any such fatal combination as being proportional to the fraction of failed subsystems; $F(t)/N$. The mortality rate in a population of such organisms will therefore also be proportional to $F(t)/N$:

$$\mu(t) \propto \frac{F(t)}{N} = \frac{F_0}{F_0 + (N - F_0)e^{-rNt}} \tag{5}$$

For living organisms we find it a plausible assumption that death occurs at relatively small fractions of failed subsystems—as stated in the fifth assumption. In this limit $F(t)$ grows exponentially with time and times are small compared to the time of inflection ($t << \tau$).

$$F(t) \approx F_0 e^{rNt} \qquad \text{for} \qquad t << \tau \tag{6}$$

In this limit we therefore obtain the Gompertzian mortality rate

$$\mu(t) \approx R_0 e^{bt} \tag{7}$$

where $b = rN$. See Fig. 2B.

An additional requirement for the model to fit empirical data is that the exponential range ($t << \tau$) is a good approximation for the entire age range that displays Gompertzian mortality, i.e., the inflection point of the logistic growth curve, τ, must be larger than the typical age range (for humans, $\tau >\sim 100$ years, but possibly much larger). Since we have, $\tau = 1/b \cdot \ln(N/F_0 - 1)$, the requirement of large τ is equivalent to requiring very small F_0/N, i.e., the fraction of failed subsystems at time zero must be very small. The model was fitted to empirical data

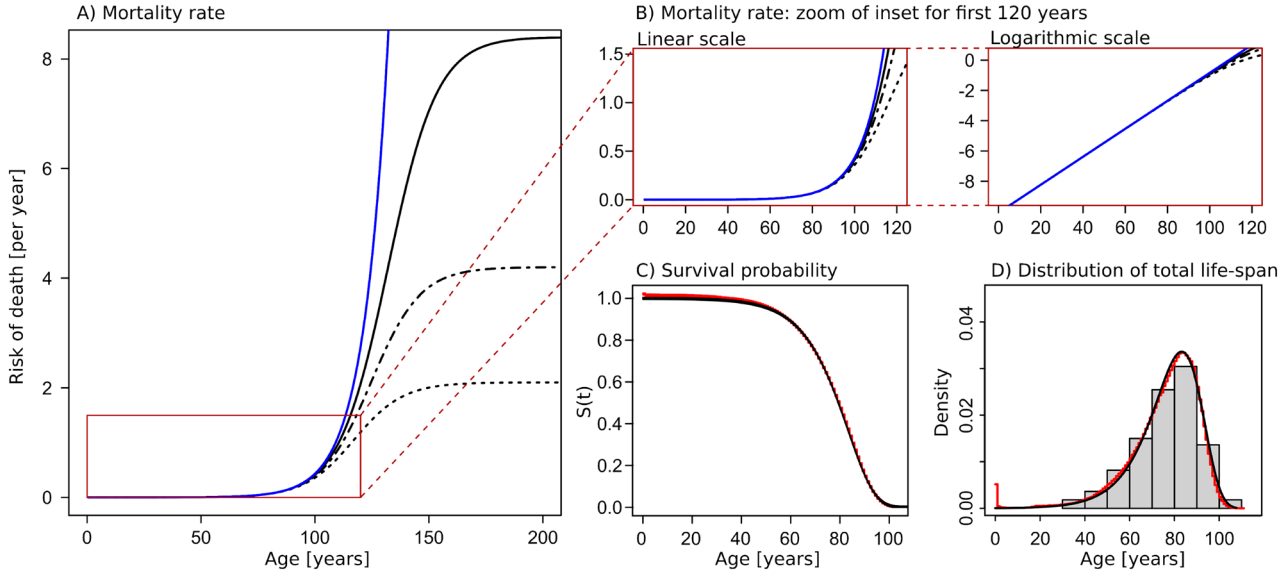

Figure 2. Gompertzian mortality emerges from logistic growth of subsystem failures. (**A**) Risk of death—equal to mortality rate on population scale—as a function of age. The blue line shows classical Gompertzian mortality (exponential increase of mortality rate with age). The three black lines show the mortality rate as predicted by the MICC model for three different choices of F_0/N (full line: $F_0/N = 1 \times 10^{-6}$, dashed-dotted line: $F_0/N = 1 \times 10^{-5}$, dashed line: $F_0/N = 2 \times 10^{-5}$). The inset marked with a red boarder corresponds to the age range which is relevant for human life-span. Within this age range the mortality rate increases approximately exponentially with age. The age range for which the exponential approximation is valid increases with decreasing values of F_0/N. Parameters used for the mean field model are: $b = 9.24 \times 10^{-3}$ per year, $R_0 = 4.2 \times 10^{-5}$ per year, $N = 10^6$, and $rN = b$. (**B**) Zoom of the relevant age-range, shown in both linear and logarithmic scale. (**C**,**D**) The survival function (**C**) and life-span distribution (**D**) corresponding to an approximately exponential mortality rate is displayed overlayed with empirical data from the Danish population—the data consists of all deaths occurring in the Danish population in the time period 1990–2019. The theoretical survival function and life-span distribution correspond to the parameter choice of $F_0/N = 1 \times 10^{-5}$.

from the Danish population, using three different choices of τ (Fig. 2A,B). The corresponding survival function and distribution of total life-span (using one specific choice of model parameters) is plotted in Fig. 2C,D, together with statistical data for all deaths occurring in Denmark in the period 1990–2019 (pooled data).

The five assumptions set up in the Introduction therefore leads to a Gompertzian mortality pattern, i.e., exponential increase of the mortality rate with age. The model also has the potential of explaining why the mortality rate deviates from the exponential increase at later times (deceleration at very old age), as the logistic growth curve starts to deviate from the exponential at ages approaching τ—see Fig. 2A,B.

N:	Total number of subsystems in one organism
$F(t)$:	The number of failed subsystems at time t, $F(t) = \frac{N \cdot F_0}{F_0 + (N - F_0)e^{-rNt}}$
$M(t)$:	The number of subsystems which are functioning correctly at time t, $M(t) = N - F(t)$
τ:	inflection point $\tau = 1/(rN) \cdot \ln(N/F_0 - 1)$, such that $F(\tau) = N/2$
$\mu(t)$:	mortality rate, $\mu(t) \propto \frac{F_0}{F_0 + (N - F_0)e^{-rNt}}$ In the limit of small fractions of failed subsystems (small $F(t)/N$): $\mu(t) \approx R_0 e^{bt}$ where $b = rN$

Multiple and inter-dependent component cause model in a *stochastic* version

While the "Mean Field model" above describes the *average* dynamics of $F(t)$, a more realistic model would be to model ΔF as a stochastic variable, allowing individual organisms to undergo individual trajectories of failure accumulation. For the individual trajectory we denote the number of failed subsystems $f_i(t)$. The number of non-failed subsystems at time t is given by $(N - f_i(t))$, and the probability, $p_i(t)$, for *each* of the subsystems to fail within the next small time-step, Δt, is proportional to the number of already failed subsystems; $p_i(t) = r \cdot f_i(t) \cdot \Delta t$. We performed a Monte Carlo simulation of stochastic subsystem failure and subsequent death, resulting in individual trajectories of $f_i(t)$, see Fig. 3A (displaying 12 individual trajectories) and Fig. 3B (displaying 220 individual trajectories).

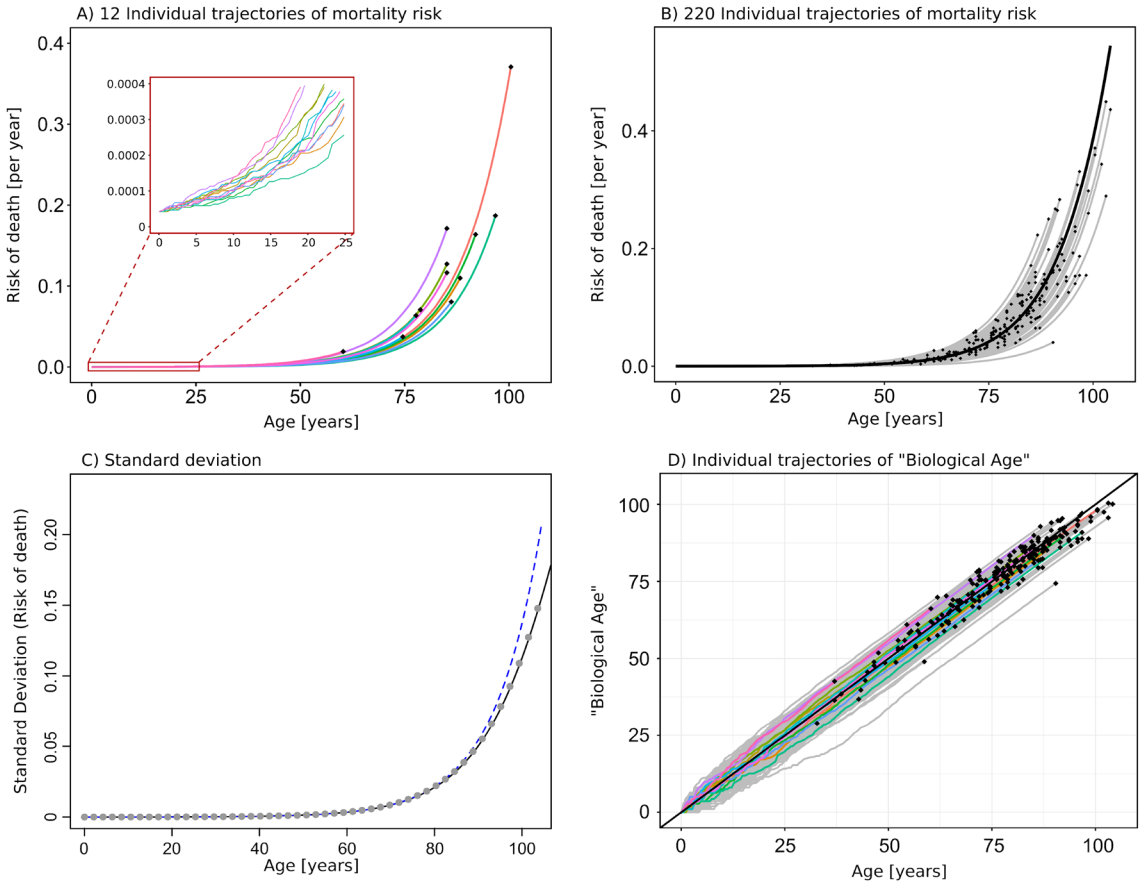

Figure 3. Individual trajectories of mortality-risk and biological age. (**A**) 12 individual trajectories of mortality risk as computed by Monte Carlo simulation. The insert displays trajectories at early ages, for which the stochastic nature of the trajectories is more clear. Black dots indicate death-events. Parameters used for the model are: $N = 10^6$, $F_0/N = 1 \times 10^{-5}$, $b = 9.24 \times 10^{-3}$ per year, $R_0 = 4.2 \times 10^{-5}$ per year, and $rN = b/0.977$ is used in order to correct for the fact that the stochastic model lags slightly compared to the mean field model (see main text and Supplemental Appendix C). (**B**) 220 individual trajectories of mortality risk are displayed together with the median (black line). Black dots indicate death-events. The corresponding distribution of total life-span (age at death) in shown in Fig. 2D. (**C**) Standard deviation (shown in grey dots) of the 220 individual trajectories shown in panel B. The black line corresponds to the approximate solution for standard deviation given by the square root of equation (11). We see that the approximate solution agrees extremely well with the simulated data. The standard deviation increases almost exponentially (an exponential curve is displayed by the blue dashed line for comparison). (**D**) Individual trajectories of "Biological age" corresponding to the 220 individual trajectories shown in panel (**B**). The colored trajectories correspond to the trajectories shown in panel (**A**). Black dots indicate death-events. Here "Biological Age" is defined as the age obtained by projection of individual values of $f_i(t)$ onto the average $\langle f \rangle$. From this plot it is clear that the timing of stochastic events at early age have large impact on the individual trajectory.

Mortality rate in the stochastic model

For the i'th individual organism, we model the probability of obtaining a fatal combination of subsystems failures as proportional to the fraction of failed subsystems, $f_i(t)/N$. The risk of death for the i'th individual organism ("individual mortality-risk") is therefore given by:

$$\mu_i(t) \propto \frac{f_i(t)}{N} \tag{8}$$

Two individuals having equal trajectories will, due to chance, not necessarily die at the exact same time, but they will share the same risk of dying at time t. The individual times of death are also computed by Monte Carlo simulation (death events are marked by black dots in Fig. 3A,B). Parameters for the simulation have been chosen to fit empirical mortality data from the Danish population, and initial conditions have been chosen to be equal for all individuals. A histogram of the total life-spans of the 220 individual trajectories shown in Fig. 3B is shown in Fig. 2D, and is seen to agree well with the analytical distribution fitted to empirical data.

The individual times of death are subject to a relatively large stochastic element, resulting from the fact that overall mortality rates are small (as determined by the empirical data). As a result, individuals of very similar mortality-risk trajectories may die at very different ages.

The individual mortality-risk trajectories display increasing variance with time, showing that some individuals have faster increasing mortality-risk than others. Below we develop a full stochastic model, describing all possible trajectories and their probability distribution as a function of time.

Average and variance of individual trajectories

In order to obtain expressions for the average and variance of many individual trajectories, we must consider the full set of all possible trajectories. An organism consisting of N subsystems can be described by $(N+1)$ different states, corresponding to $f_i = \{0, 1, 2, \ldots, N\}$ failed subsystems and $(N - f_i)$ non-failed subsystems. Note that we only describe the *number* of failed subsystems, but do not discriminate between different combinations of failures, nor do we discriminate between different orders of obtaining the subsystems failures.

We define $P(f, t)$ as the probability of having exactly f failed subsystems at time t, and derive an expression for the time evolution of $P(f, t)$. The *master equation* for $\frac{d}{dt}P(f,t)$ may be expressed in two terms: one term describing the risk of *transitioning* from $(f-1)$ to f failed subsystems, and one term describing the risk of *transitioning* from f to $(f+1)$ failed subsystems. Following the same logic as for the mean field model, the risk of experiencing another subsystem failure within an infinitesimal time-step—and hence make a transition from one state to the next—is proportional to $r \cdot (N - f_i) \cdot f_i$. We therefore have the following expression for the master equation:

$$\frac{d}{dt}P(f,t) = r(N-f+1)(f-1)P(f-1,t) - r(N-f)fP(f,t). \tag{9}$$

An approximate analytical solution to Eq. (9) may be obtained by performing Van Kampen's system size expansion[39] (i.e., the limit of very large N) and using Linear Noise Approximation (LNA) to obtain expressions for the average, $\langle f(t)\rangle$, and variance, $\langle (f(t) - \langle f(t)\rangle)^2\rangle$, as functions of time. See Supplemental Appendix B for details of the derivation. The approximate solution to Eq. (9) confirms that the average behaves as the mean field model described above; a logistic growth curve, which displays exponential growth for times $t << \tau$.

$$\langle f(t)\rangle = \frac{Nf_0}{f_0 + (N - f_0)e^{-rNt}} \tag{10}$$

The solution to $\langle f(t)\rangle$ is therefore equal to the mean field solutions shown in Fig. 2A,B.

The approximate solution to Eq. (9) also provides an analytical expression for the variance $\langle (f(t) - \langle f(t)\rangle)^2\rangle = N \cdot \Xi(t)$. A general solution for $\Xi(t)$ is given in Supplemental Appendix B. Here we provide the solution for the special case where $\Xi(0) = 0$ (zero variance at time $t = 0$) in the limit $t << \tau$:

$$\langle (f(t) - \langle f(t)\rangle)^2\rangle \approx f_0 e^{2rNt}\left(1 - e^{-rNt}\right) \tag{11}$$

In Fig. 3C, the analytical solution given by Eq. (11) is plotted together with the variance of 220 individual mortality-risk trajectories computed by Monte Carlo simulation. The results reveal that the variance of individual trajectories increases almost exponentially with age (exponential growth is plotted for comparison), but that the variance grows slower than exponential for more advanced ages. We note that the variance computed from the Monte Carlo simulations corresponds to the variance of 220 trajectories in the case where death events are ignored, such that right censoring of data is avoided.

The individual trajectories shown in Fig. 3A,B indicate that the "fate" of an individual trajectory is largely determined by stochastic events in early life. At more advanced ages trajectories rarely cross. Another way to represent this dependence on events in early age is to display the individual trajectories in terms of a measure of "Biological age". We relate the individual trajectories of subsystem failure ($f_i(t)$) to a measure of "Biological Age" by projecting the individual values of $f_i(t)$ onto the mean field average, see Fig. 3D. The construction of such a "Biological Age" provides an alternative but equally valid representation of the individual trajectories of mortality risk. The individual trajectories of "Biological Age" are largely determined by stochastic events in early life—at more advanced ages the trajectories become close to linear.

Full numerical solution reveals stochastic effects

In order to compute the full distribution of $P(f, t)$ for a finite value of the parameter N, we derive an expression that may be solved numerically for discrete time. The derivation is given in Supplemental Appendix C. Calculation of the full distribution of $P(f, t)$ reveals that the distribution is asymmetric and right-skewed at early times such that the average is slightly higher than the median. The asymmetry becomes more pronounced for smaller values of the parameter N (see Supplementary Fig. 1A in Supplemental Appendix C). As we need to choose a relatively large value for N in order to fit the empirical data for human mortality, the asymmetry is not very pronounced in the plots shown in Fig. 3A,B.

The calculations also reveal that the average and median of the stochastic model displays a small time-lag compared to the mean-field model (see Supplementary Fig. 1B in Supplemental Appendix C). This stochastic effect means that the individual trajectories grow slightly slower than expected from the mean-field model and that the parameter r used in the stochastic model should therefore be slightly adjusted in order to fit the empirical data. Exact values for all simulations is given in the figure captions.

Model alterations: spontaneous failure and repair mechanism

It is possible to alter the model to incorporate a small risk of spontaneous subsystem failure in addition to the inter-dependent subsystem failure. In this case we have $p_i(t) = (r \cdot f_i(t) + r\epsilon N) \cdot \Delta t$, where ϵ is small. If ϵN is of same order as f_0, then the term proportional to f_i will very quickly start to dominate and the model is still

able to produce Gompertzian mortality. However, if ϵN is much larger than f_0 then the term proportional to ϵ will dominate and the increase in $f_i(t)$ will not display Gompertzian mortality, but instead resemble the situation with constant subsystem failure-rate as described in Supplemental Appendix A.

Another possible alteration of the model is to incorporate a repair mechanism, making it possible for failed subsystems to reverse back to the non-failed state. If the repair mechanism is spontaneous, and given by the rate parameter α, then the rate equation for the corresponding mean-field model is

$$\begin{aligned}\frac{dF(t)}{dt} &= r \cdot F(t)(N - F(t)) - \alpha F(t) \\ &= r \cdot F(t)(N - \alpha/r - F(t))\end{aligned}$$

Thus the resulting model is still able to produce Gompertzian mortality, but the parameter N, should be substituted by $(N - \alpha/r)$.

Discussion

Within the broad field of aging research there exists an ongoing nonconsensus regarding the definition of the aging process itself[2]. Many researchers have attempted to set up defining paradigms, uncover molecular biomarkers and pathways, and construct mathematical models, all aiming to capture the essential aging process and possibly to quantify it[1,4,5,40–42]. It has recently been argued that we may enrich our general understanding of aging by shifting focus towards interactions occurring on multiple hierarchical scales ranging from molecular to clinical[1,9,10], as opposed to focusing solely on cellular and molecular scales. Although all biology is ultimately dependent on interacting molecules, many functionalities only emerge on larger scales, where several molecules, cells, tissues and organs interact in self-organising synergy. Functionalities that emerge on larger scales are not easily understood through a focus on individual molecular interactions but necessitate a shift in perspective towards a more coarse grained understanding of phenomenological mechanisms. Here we define simple laws (assumptions) that explain the overall mortality pattern termed Gompertzian mortality. As an analogy consider the planetary movements, which were described by Kepler's Laws of planetary motion in the early 1600s, and later even better understood by Newton's Laws of motion. Both Kepler's and Newton's Laws ignores many details—e.g., detailed appearance and material composition of the different planets—and aims to set up simple laws that explain the overall movement in sufficient detail.

Building on modern epidemiological theory[33], viewing mortality as a "*sufficient cause*" comprised of its variable "*component causes*", we propose that the process of aging can be described as the accumulation of inter-dependent subsystem failures. We show the model is able to explain the emergence of Gompertzian mortality with only five simple assumptions, which seems both reasonable and sufficiently general to be applicable to many different species. These assumptions have the advantage that they do not relate to specific cellular or molecular pathways. A key assumption driving the accelerated increase in mortality risk is the inter-dependency between subsystems and the second assumption of the model stating that—on average—failure of one subsystem leads to an increased risk of failure within other subsystems. Inter-dependencies between subsystems agree extremely well with empirical data, wherein significant increases in hazard rates are observed for outcomes related to numerous relevant exposures.

The MICC model serves to explain overall driving mechanisms of aging, and allows for different aging trajectories to be contained within this framework. While Rothman's *Sufficient-Component Cause Model*[33] is deterministic in its set-up, the MICC model adds stochasticity in terms of the individual trajectories of subsystem failures.

The model is extendable to outcomes other than death. Age-related diseases may also be described as endpoints that are attained by different combinations of subsystem failures. Hence the model also explains why complex, non-communicable diseases display incidence rates that increase exponentially with age[17,18]. The detailed structure of different aging trajectories, possibly involving disease manifestation, are structures that share similar overall kinetics of aging, but relate to different combinations of subsystem failures all of which contribute to mortality risk. A possible extension of our proposed model is to assume that not all subsystems are equally dependent and that there may exist clusters of highly inter-dependent subsystems with a correlation structure. The model introduced in this paper represents the basic case of a fully connected and uniformly weighted network. The network structure of our model could easily be extended to include a modular structure or a scale-free structure as proposed by Rutenberg et al.[5]. Both network models would be highly relevant: scale-free networks are found in many natural systems[32] and modular networks are also found in many biological systems[43]—organs are simple examples of a highly modular structure. In Fig. 4, we visually show a simple example of how one could incorporate a highly modular structure by compartmentalising the many subsystems into *clusters* of highly connected subsystems. In this example, one cluster represents the cardiovascular system, another cluster represents the respiratory system and so forth. It would then be straightforward to assume that subsystems *within* the same cluster would be highly inter-dependent (failure of one subsystem would considerably increase the risk of failure for fellow subsystems), while subsystems from *different* clusters might not be very inter-dependent or not inter-dependent at all (failure of a subsystem in one cluster would not increase the risk of subsystems in other clusters). However, we would then expect that certain subsystems would serve as connections between different clusters and therefore—on average—any subsystem failure could eventually increase the risk for other subsystem failures. We hypothesize that the subsystems (network-nodes) that act as connectors between clusters (network modules) would be prime targets for intervention in order to reduce the pace of damage accumulation.

The detailed network structure of inter-dependencies described above and represented by Fig. 4 would lead to clusters in individual failure trajectories. Such clusters of failure trajectories could represent different diseases and individual trajectories that fall within these clusters would represent persons that have the same disease although slightly different manifestations of it. Recent studies confirm the presence of a multiorgan aging network, in

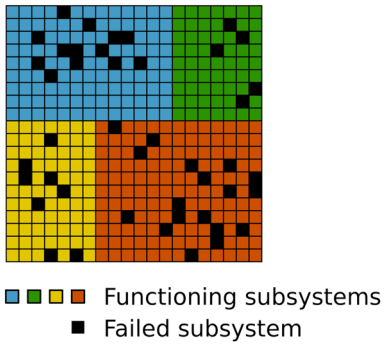

Figure 4. Clustering of subsystems within the complex organism. A possible extension of the model would be to attribute each subsystem to certain compartments or *clusters* (indicated by different colors) of highly connected subsystems that relate to higher order of organizational functionalities, e.g. one cluster represents the cardiovascular system, another cluster represents the respiratory system and so forth.

which the biological age of organs selectively influences the aging of other organ systems[44]. The uncovering of this network structure is of the essence in order to understand how living systems function. Future work could extend the MICC framework to explore how interventions designed to prevent failure will affect the overall aging of the organism and possibly modulate aging trajectories. Deeper understanding of such structures would be valuable for understanding the progression of specific aging phenotypes as well as for elucidating possible targets for intervention in order to prolong health-span through counteracting disease progression.

As we have shown here, a detailed network structure is not necessary for explaining the emergence of Gompertzian mortality. The MICC model is able to robustly produce Gompertzian mortality patterns as long as the number of subsystems is large enough to allow for the exponential range to span an appropriate age range—for the case of human mortality the age range is of the order of 100 years. By fitting the model to empirical data for human mortality we arrive at values of N (system size) of order 10^6 (see Fig. 2A and caption). The robust emergence of Gompertzian mortality patterns agrees well with the empirical observations across many species. The MICC model implies that Gompertzian mortality patterns will emerge in large systems consisting of inter-dependent subsystems—this would include many (if not all) biological species, and is also able to explain why the Gompertz Law also holds for complex computer code.

Ethical approval

Human participants are only passively involved through national register data, which does not require approval from ethics committee. Approval to use register data was granted by Statistics Denmark and the Danish Health Data Authority.

Patient and public involvement

Patients and/or the public were not involved in the design, or conduct, or reporting, or dissemination plans of this research.

Data availibility

The life-span data for the Danish population 1990–2019 (see Fig. 2C,D) is available in a supplementary file included in this publication. The simulated data for trajectories of mortality-risk (see Fig. 3) are available from the corresponding author on reasonable request.

Received: 8 September 2023; Accepted: 8 January 2024
Published online: 12 January 2024

References

1. Zierer, J., Menni, C., Kastenmüller, G. & Spector, T. D. Integration of 'omics' data in aging research: From biomarkers to systems biology. *Aging Cell* **14**, 933–944. https://doi.org/10.1111/acel.12386 (2015).
2. Cohen, A. A. *et al.* Lack of consensus on an aging biology paradigm? A global survey reveals an agreement to disagree, and the need for an interdisciplinary framework. *Mech. Ageing Dev.* **191**, 111316. https://doi.org/10.1016/j.mad.2020.111316 (2020).
3. Palmer, R. D. Aging clocks and mortality timers, methylation, glycomic, telomeric and more. A window to measuring biological age. *Aging Med.* **5**, 120–125. https://doi.org/10.1002/agm2.12197 (2022).
4. Jylhävä, J., Pedersen, N. L. & Hägg, S. Biological age predictors. *EBioMedicine* **21**, 29–36. https://doi.org/10.1016/j.ebiom.2017.03.046 (2017).
5. Rutenberg, A. D., Mitnitski, A. B., Farrell, S. G. & Rockwood, K. Unifying aging and frailty through complex dynamical networks. *Exp. Gerontol.* **107**, 126–129. https://doi.org/10.1016/j.exger.2017.08.027 (2018).
6. Farrell, S. G., Mitnitski, A. B., Theou, O., Rockwood, K. & Rutenberg, A. D. Probing the network structure of health deficits in human aging. *Phys. Rev. E* **98**, 032302. https://doi.org/10.1103/PhysRevE.98.032302 (2018).
7. Mitnitski, A. B., Rutenberg, A. D., Farrell, S. & Rockwood, K. Aging, frailty and complex networks. *Biogerontology* **18**, 433–446. https://doi.org/10.1007/s10522-017-9684-x (2017).

8. Klemera, P. & Doubal, S. A new approach to the concept and computation of biological age. *Mech. Ageing Dev.* **127**, 240–248. https://doi.org/10.1016/j.mad.2005.10.004 (2006).
9. Cohen, A. A., Legault, V. & Fülöp, T. What if there's no such thing as "aging"?. *Mech. Ageing Dev.* **192**, 111344. https://doi.org/10.1016/j.mad.2020.111344 (2020).
10. Cohen, A. A. *et al.* A complex systems approach to aging biology. *Nat. Aging* **2**, 580–591. https://doi.org/10.1038/s43587-022-00252-6 (2022).
11. Gompertz, B. On the nature of the function expressive of the law of human mortality, and on a new mode of determining the value of life contingencies. *Philos. Trans. R. Soc.* **2**, 513–585 (1825).
12. Finch, C. E. *Longevity, Senescence, and the Genome* (The University of Chicago Press, 1990).
13. Olshansky, S. J. & Carnes, B. A. Ever since Gompertz. *Demography* **34**, 1–15. https://doi.org/10.2307/2061656 (1997).
14. Beard, R. E. *Appendix: Note on Some Mathematical Mortality Models* 302–311 (Wiley, 1959). https://doi.org/10.1002/9780470715253.app1.
15. Yashin, A. I., Stallard, E. & Land, K. C. *Biodemography of Aging: Determinants of Healthy Life Span and Longevity* (Springer, 2017).
16. Strehler, B. L. & Mildvan, A. S. General theory of mortality and aging. *Science* **132**, 14–21. https://doi.org/10.1126/science.132.3418.14 (1960).
17. Belikov, A. V. Age-related diseases as vicious cycles. *Ageing Res. Rev.* **49**, 11–26. https://doi.org/10.1016/j.arr.2018.11.002 (2019).
18. Zenin, A. *et al.* Identification of 12 genetic loci associated with human healthspan. *Commun. Biol.* **2**, 41. https://doi.org/10.1038/s42003-019-0290-0 (2019).
19. Katzir, I. *et al.* Senescent cells and the incidence of age-related diseases. *Aging Cell* **20**, e13314. https://doi.org/10.1111/acel.13314 (2021).
20. Navaratnam, V. *et al.* The rising incidence of idiopathic pulmonary fibrosis in the UK. *Thorax* **66**, 462–467. https://doi.org/10.1136/thx.2010.148031 (2011).
21. Oliveria, S. A., Felson, D. T., Reed, J. I., Cirillo, P. A. & Walker, A. M. Incidence of symptomatic hand, hip, and knee osteoarthritis among patients in a health maintenance organization. *Arthritis Rheumatism* **38**, 1134–1141. https://doi.org/10.1002/art.1780380817 (1995).
22. Ohishi, K., Okamura, H. & Dohi, T. Gompertz software reliability model: Estimation algorithm and empirical validation. *J. Syst. Softw.* **82**, 535–543. https://doi.org/10.1016/j.jss.2008.11.840 (2009).
23. Tishby, I., Biham, O. & Katzav, E. The distribution of path lengths of self avoiding walks on erds-rényi networks. *J. Phys. A Math. Theor.* **49**, 285002. https://doi.org/10.1088/1751-8113/49/28/285002 (2016).
24. Jones, O. R. *et al.* Diversity of ageing across the tree of life. *Nature* **505**, 169–173. https://doi.org/10.1038/nature12789 (2014).
25. Gavrilov, L. A. & Gavrilova, N. S. The reliability theory of aging and longevity. *J. Theor. Biol.* **213**, 527–545. https://doi.org/10.1006/jtbi.2001.2430 (2001).
26. Vaupel, J. W. *et al.* Biodemographic trajectories of longevity. *Science* **280**, 855–860. https://doi.org/10.1126/science.280.5365.855 (1998).
27. Anderson, J. J. A vitality-based model relating stressors and environmental properties to organism survival. *Ecol. Monogr.* **70**, 445 (2000).
28. Arbeev, K. G. *et al.* Age trajectories of physiological indices in relation to healthy life course. *Mech. Ageing Dev.* **132**, 93–102. https://doi.org/10.1016/j.mad.2011.01.001 (2011).
29. Karin, O., Agrawal, A., Porat, Z., Krizhanovsky, V. & Alon, U. Senescent cell turnover slows with age providing an explanation for the Gompertz law. *Nat. Commun.* **10**, 5495 (2019).
30. Ledberg, A. Exponential increase in mortality with age is a generic property of a simple model system of damage accumulation and death. *PLoS One* **15**, 1–17. https://doi.org/10.1371/journal.pone.0233384 (2020).
31. Barabási, A.-L., Gulbahce, N. & Loscalzo, J. Network medicine: A network-based approach to human disease. *Nat. Rev. Genet.* **12**, 56–68. https://doi.org/10.1038/nrg2918 (2011).
32. Cohen, R. & Havlin, S. *Complex Networks: Structure, Robustness and Function* Vol. 1 (Cambridge University Press, 2010).
33. Rothman, K. J. *et al. Modern Epidemiology* Vol. 3 (Wolters Kluwer Health, 2008).
34. Holm, N. N., Frølich, A., Andersen, O., Juul-Larsen, H. G. & Stockmarr, A. Longitudinal models for the progression of disease portfolios in a nationwide chronic heart disease population. *PLoS One* **18**, 1–26. https://doi.org/10.1371/journal.pone.0284496 (2023).
35. Rothman, K. J. Causes. *Am. J. Epidemiol.* **104**, 587–592. https://doi.org/10.1093/oxfordjournals.aje.a112335 (1976).
36. Partridge, L. & Mangel, M. Messages from mortality: The evolution of death rates in the old. *Trends Ecol. Evol.* **14**, 438–442. https://doi.org/10.1016/S0169-5347(99)01646-8 (1999).
37. Khazaeli, A. A. Effect of density on age-specific mortality in drosophila: A density supplementation experiment. *Genetica* **98**, 21–31. https://doi.org/10.1007/BF00120215 (1996) (**Cited by: 34.**).
38. Fukui, H., Xiu, L. & Curtsinger, J. W. Slowing of age-specific mortality rates in drosophila melanogaster. *Exp. Gerontol.* **28**, 585–599. https://doi.org/10.1016/0531-5565(93)90048-I (1993).
39. Van Kampen, N. G. *Stochastic Processes in Physics and Chemistry* Vol. 1 (Elsevier, 1992).
40. López-Otín, C., Blasco, M. A., Partridge, L., Serrano, M. & Kroemer, G. The hallmarks of aging. *Cell* **153**, 1194–1217. https://doi.org/10.1016/j.cell.2013.05.039 (2013).
41. Schmauck-Medina, T. *et al.* New hallmarks of ageing: A 2022 Copenhagen ageing meeting summary. *Aging* **14**, 6829–6839. https://doi.org/10.18632/aging.204248 (2022).
42. Arbeev, K. G., Ukraintseva, S. V. & Yashin, A. I. Dynamics of biomarkers in relation to aging and mortality. *Mech. Ageing Dev.* **156**, 42–54. https://doi.org/10.1016/j.mad.2016.04.010 (2016).
43. Kashtan, N. & Alon, U. Spontaneous evolution of modularity and network motifs. *Proc. Natl. Acad. Sci.* **102**, 13773–13778. https://doi.org/10.1073/pnas.0503610102 (2005).
44. Tian, Y. E. *et al.* Heterogeneous aging across multiple organ systems and prediction of chronic disease and mortality. *Nat. Med.*https://doi.org/10.1038/s41591-023-02296-6 *(2023).*

Acknowledgements

We wish to thank professor Rudi J. Westendorp for interesting discussions and perspectives, and for supporting the development of the model at early stages. We also thank Héléne Toinét Cronjé and Rebecca Bolt Ettlinger for critically revising the manuscript and giving valuable feedback.

Author contributions

P.Y.N. developed the model, performed all simulations, and wrote the original draft. N.M. performed the mathematical analysis providing the approximate analytical solution to the stochastic system. P.Y.N., M.K.J., N.M. and S.B. contributed to the writing of the manuscript. All authors have critically revised and approved the final version.

Funding
The study was funded by the Novo Nordisk Challenge Programme [NNF17OC0027812]. S.B. acknowledges funding from the MRC Centre for Global Infectious Disease Analysis (reference MR/X020258/1), funded by the UK Medical Research Council (MRC). This UK funded award is carried out in the frame of the Global Health EDCTP3 Joint Undertaking. S.B. acknowledges support from the National Institute for Health and Care Research (NIHR) via the Health Protection Research Unit in Modelling and Health Economics, which is a partnership between the UK Health Security Agency (UKHSA), Imperial College London, and the London School of Hygiene &; Tropical Medicine (grant code NIHR200908). (The views expressed are those of the authors and not necessarily those of the UK Department of Health and Social Care, NIHR, or UKHSA.). S.B. acknowledges support from the Novo Nordisk Foundation via The Novo Nordisk Young Investigator Award (NNF20OC0059309). S.B. acknowledges the Danish National Research Foundation (DNRF160) through the chair grant. S.B. acknowledges support from The Eric and Wendy Schmidt Fund For Strategic Innovation via the Schmidt Polymath Award (G-22-63345).

Competing interests
The authors declare no competing interests.

Additional information
Supplementary Information The online version contains supplementary material available at https://doi.org/10.1038/s41598-024-51669-5.

Correspondence and requests for materials should be addressed to P.Y.N.